Computational electrocatalysis: methods and fundamental applications on CO2 reduction and formic acid oxidation

Granda Marulanda, L.P.

Oudegracht
Utrecht, The Netherlands

5 Adsorption Processes on a Pd-Monolayer-Modified Pt(111) Electrode

Specific adsorption of anions is an important aspect in surface electrochemistry in view of its influence on reaction kinetics as either a promoter or an inhibitor. Perchloric acid is typically considered as an ideal electrolyte for investigating electrocatalytic reactions due to the lack of specific adsorption of the perchlorate anion on several metal electrodes. In this work, cyclic voltammetry and computational methods are combined to investigate the interfacial processes on a Pd monolayer deposited on Pt(111) single crystal electrodes in perchloric acid solution. The "hydrogen region" of this $Pd_{ML}Pt(111)$ surface exhibits two voltammetric peaks: the first "hydrogen peak" at 0.246 V vs RHE involves the replacement of hydrogen by hydroxyl, and the second "hydrogen peak" H_{II} at 0.306 V vs RHE appears to be the replacement of adsorbed hydroxyl by specific perchlorate adsorption. The two peaks merge into a single peak when a more strongly adsorbed anion, such as sulfate, is involved. Our density functional theory calculations qualitatively support the peak assignment and show that anions generally bind more strongly to the $Pd_{ML}Pt(111)$ surface than to Pt(111).

This chapter is based on Chen, X.; Granda-Marulanda, L. P.; McCrum, I. T.; Koper, M. T. M. Adsorption Processes on a Pd Monolayer-Modified Pt(111) Electrode. Chem. Sci. 2020, 11 (6), 1703–1713. Also published in Chen, X. Adsorption and Catalysis on Pt and Pd Monolayer-Modified Pt Single Crystal Electrodes, PhD thesis, Leiden University, 2019- Chapter 4

All experiments were performed by Xiaoting Chen.

5.1 Introduction

Improved understanding of electrocatalytic reactions taking place in various energy storage and energy conversion devices becomes increasingly crucial with the advent of electrochemical fuel production and fuel-cell technologies. For many relevant electrocatalytic reactions, such as the hydrogen oxidation reaction (HOR), the oxygen reduction reaction (ORR), the formic acid oxidation, and the CO_2 reduction reaction, not only the surface structure but also the adsorption of anions/cations from the supporting electrolyte influence the reactivity through different interactions of these co-adsorbates with key reaction intermediates.[1–3] For instance, hydrogen (*H) and hydroxyl (*OH) are important surface-bonded intermediates during the aforementioned reactions. In previous works, we showed that cations co-adsorb with hydroxyl species on the step sites of Pt electrodes at low potentials, and that the corresponding cation-hydroxyl interaction is responsible for the non-Nernstian pH shift, a shift due to the weakened adsorption of *OH by the cation on the surface, of the step-related voltammetric peak.[4,5]

Platinum is one of the most important catalysts due to its widespread application in heterogeneous catalysis and electrochemistry. There have been plenty of studies on single-crystal platinum electrodes since the preparation method of clean platinum surfaces introduced by Clavilier.[6] Palladium is a platinum-group metal and similar to Pt in many chemical and physical properties. Interestingly, Pd surfaces show a higher activity toward formic acid oxidation than Pt, but the most remarkable difference with Pt is the absence of CO poisoning during formic acid oxidation on Pd.[7–9] Moreover, Pd electrodes have attracted increasing attention as catalysts for the CO_2 electroreduction reaction, as they selectively reduce CO_2 to formic acid with low overpotential,[10,11] implying that Pd is an (almost) reversible catalyst for the conversion of formic acid to carbon dioxide and vice versa.[12]

To better understand the special reactivity of palladium, detailed investigations on atomically well-defined Pd surfaces are highly desirable. However, the electrochemistry of well-defined Pd surfaces is not as well studied as for Pt surfaces, which arises partially from the difficulty to prepare Pd single crystals as well as from the effect that palladium absorbs substantial amounts of hydrogen below 0.2 V vs RHE, masking other reactions taking place on its surface.[13] Epitaxially grown Pd layers on a foreign metal are a promising alternative and have attracted considerable attention, particularly Pt(111) surfaces modified by a Pd monolayer.[14–17] The lattice parameters of both metals are close, 3.89 Å for Pd and 3.92 Å for Pt, and it has been pointed out that the reactivity of the Pd monolayer system is comparable to that of the corresponding Pd single crystal.[18,19]

To understand the fundamental aspects of the electrode activity, we need to consider the adsorption behavior on single-crystal electrodes in acid electrolyte solutions. Particularly interesting are perchloric and sulfuric acid solutions, especially in relation to specific anion adsorption. In sulfuric acid, the $Pd_{ML}Pt(111)$ electrode has been studied by spectroelectrochemical experiments, showing that the majority of species on the surface are hydrogen at low potential and (bi)sulfate[20] at high potential. Remarkably, a reversible double peak adsorption state appears in the hydrogen region of the voltammogram of a $Pd_{ML}Pt(111)$ in

0.1 M $HClO_4$. Previous studies in a low potential window (0.05-0.35 V vs RHE) have ascribed these peaks to hydrogen underpotential deposition (H_{upd}) because a hydrogen coverage of 1 H_{upd} per Pd corresponds very well to the total charge under these two peaks (240 μ C cm^{-2}).[21,22] However, the double-peak nature of this "hydrogen region" of $Pd_{ML}Pt(111)$ remains unresolved.

In this ***Chapter***, we use a combination of experimental and computational methods for the elucidation of the surface species formed on the well-defined $Pd_{ML}Pt(111)$ surface in the so-called "hydrogen region". We argue that in perchloric acid solution, the "hydrogen region" on the $Pd_{ML}Pt(111)$ surface is rather a "hydrogen-hydroxyl-cation-anion region". We show the existence of cation and anion effects on the peaks in the "hydrogen region", showing that OH and anions interact much more strongly with the $Pd_{ML}Pt(111)$ surface than with the Pt(111) surface.

These results improve our fundamental understanding of anion, cation and OH adsorption on well-defined, single-crystal palladium surfaces, which will be important for interpreting and tuning the catalytic activity of palladium-based electrochemical interfaces.

5.2 Experimental Details

Cyclic voltammetry measurements were carried out in standard electrochemical cells using a three-electrode assembly at room temperature. Experiments were performed in a fluorinated ethylene propylene (PEP, Nalgene) electrochemical cell for hydrofluoric acid, whereas a glass cell was used for the other electrolytes. All glassware was cleaned in an acidic solution of potassium permanganate overnight, followed by rinsing with an acidic solution of hydrogen peroxide and repetitive rinsing and boiling with ultrapure water. A Pt(111) bead-type electrode, with a diameter of 2.27 mm, was used as working electrode. Prior to each experiment, the working electrode was prepared according to the Clavilier method.[6] A platinum wire was used as counter electrode and a reversible hydrogen electrode (RHE) was employed as the reference electrode, in a separate compartment filled with the same electrolyte, at the same pH as the electrolyte in the electrochemical cell. All potentials are reported versus the RHE. The electrochemical measurements were performed with the single-crystal electrode in the hanging meniscus configuration. The potential was controlled with an Autolab PGSTAT302N potentiostat. The current density shown in the manuscript represents the measured current normalized to the geometric area of the working electrode.

The Pd monolayer in this study was prepared using a method similar to the one reported before.[17,20] The freshly prepared Pt(111) electrode was immersed into the Pd^{2+} containing solution at 0.85 V vs RHE , where no Pd deposition occurred, and the potential was continuously cycled between 0.07 and 0.85 V vs RHE at 50 mV s^{-1}. The amount of palladium on the surface was monitored by following the evolution of the voltammetric peak at 0.23 V vs RHE (as shown in Figure D1), characteristic of the presence of Pd adatoms, the charge (and current density) of which depend on the palladium coverage.[17,23] Scanning tunnelling microscopy (STM) images have revealed that monoatomic high Pd islands nucleate on the Pt(111) surface with no noticeable preference for nucleation sites, and that a full Pd monolayer without detectable holes is formed after deposition.[24] STM also

shows the presence of an ordered sulphate adlayer with a √3×√9)R19.1° structure on the Pd monolayer, as is also the case for the Pd(111) surface.[25] After Pd modification, the $Pd_{ML}Pt(111)$ electrode was taken from the cell and thoroughly rinsed with ultrapure water before performing further electrochemistry tests. Further insight into the nature of the adsorbed species on the electrode was obtained by means of charge displacement experiments using CO (Linde 6.0) as a neutral probe. The procedure to perform CO displacement measurements is similar to the one reported before.[26] Briefly, a gaseous CO stream was dosed at a fixed potential and a transient current was recorded until the $Pd_{ML}Pt(111)$ surface was covered by a monolayer of CO.

Electrolytes were made from ultrapure water (Milli-Q, 18.2 MΩ cm), high purity reagents $HClO_4$ (70%), H_2SO_4(96%), $NaClO_4$ (99.99%), CH_3SO_3H (>99.0%) and HF (40%) from Merck Suprapur and HCl, $PdSO_4$ (99.99%), $LiClO_4$ (99.99%) from Aldrich Ultrapure. Before each experiment, the electrolytes were first purged with argon (Air Products, 5.7) for at least 30 min to remove air from the solution.

5.3 Computational Details

To better understand adsorption phenomena on the $Pd_{ML}Pt(111)$ electrode, we have evaluated the free energies of adsorption of hydrogen, oxygen, hydroxide, and different anions on Pt(111), and $Pd_{ML}Pt(111)$ using Density Functional Theory (DFT) calculations. The potential-dependent free energies of adsorption of hydrogen, oxygen, hydroxide were calculated at different surface coverages using the computational hydrogen electrode.[27] By calculating the free energies of adsorption at different coverages we can determine the composition of the electrode surface in the electrochemical environment, which is useful for fundamental studies of electrocatalysis.[19,28,29]

Additionally, we calculated the potential-dependent free energies of adsorption of other anions, namely, perchlorate, sulfate and bisulfate using an alternative computational reference method as outlined in detail in ***Chapter 3***. The relative binding strength of bicarbonate and fluoride at a coverage of 1/9 ML was also calculated to compare the interaction of different anions on both surfaces. Plotting the adsorption free energy as a function of coverage and electrochemical potential allows for direct comparison with experimentally measured cyclic voltammograms, providing information on the identity and the relevant coverage of the species adsorbed on the surface at a particular potential (where peaks in current in the experimental CV correspond to changes in adsorbate coverage and/or identity). Further information on the DFT methods employed in this ***Chapter*** can be found in Appendix D.

5.4 Results and discussion

5.4.1 Comparison of the blank voltammograms of $Pd_{ML}Pt(111)$ and Pt(111)

The cyclic voltammogram of $Pd_{ML}Pt(111)$ in 0.1 M H_2SO_4 shows the presence of a sharp pair of peaks (Figure 5.1a), slightly irreversible, with a peak potential of 0.23 V vs RHE in the positive-going scan and of 0.21 V vs RHE in the negative-going scan. The sharpness of the peak suggests the replacement of adsorbed species, i.e. hydrogen and (bi)sulphate, as a function of potential.[30,31] Note that on Pt(111), hydrogen adsorption/desorption and (bi)sulphate adsorption/desorption give rise to separate voltammetric signals (between 0.05 and 0.30 V vs RHE and between 0.30 and 0.55 V vs RHE , respectively). This single sharp peak observed on the $Pd_{ML}Pt(111)$ surface can be explained by the replacement of adsorbed hydrogen at potentials below 0.22 V vs RHE by adsorbed (bi)sulphate at potentials above 0.22 V vs RHE , caused by the stronger (bi)sulphate adsorption on $Pd_{ML}Pt(111)$ compared to Pt(111).

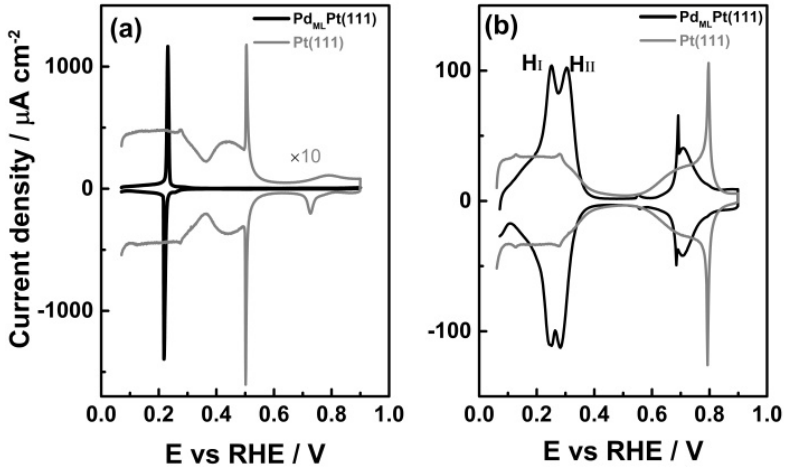

FIGURE 5.1

Cyclic voltammograms of $Pd_{ML}Pt(111)$ in (a) 0.1 M H_2SO_4 and (b) 0.1 M $HClO_4$ recorded at 50 mV s^{-1}. The blank voltammograms for Pt(111) recorded under identical conditions are shown for comparison.

Figure 5.1b shows the cyclic voltammogram of $Pd_{ML}Pt(111)$ in 0.1 M $HClO_4$ electrolyte, compared to Pt(111). The $Pd_{ML}Pt(111)$ electrode exhibits characteristic windows in the same potential regions of 0.05-0.35 V vs RHE, 0.35-0.60 V vs RHE and 0.60-0.90 V vs RHE as Pt(111). This led previous authors to conclude that the voltammetric peaks between 0.05-0.35 V vs RHE correspond to hydrogen adsorption, that the 0.35-0.60 V vs RHE is the double layer region, and that OH adsorbs in the 0.60-0.90 V vs RHE window.[21] However, there are some important differences. The first effect of the Pd ML is an increase of the overall charge

between 0.05-0.35 V vs RHE from 160 μC cm^{-2} for bare Pt(111) to 240 μC cm^{-2} for a full monolayer of Pd decorating the Pt(111). The groups of Feliu[21] and Markovic[22] ascribed the higher charge of the reversible peak in the low potential window to H_{upd} on Pd monolayer due to a stronger H_{upd}-$Pd_{ML}Pt(111)$ interaction compared to the H_{upd}-Pt(111) interaction, and to the excellent correspondence to a full monolayer of hydrogen (1 ML of one monovalent adsorbate adsorbed per surface atom, or 1.5×10^{15} atoms cm^{-2}, is exactly 240 μC cm^{-2}). Secondly, the "hydrogen region" features two sharp peaks, indicated as the "first hydrogen peak" H_I and "second hydrogen peak" H_{II} (at 0.25 and 0.30 V vs RHE, respectively), which is in contrast with the characteristic behavior of hydrogen adsorption on wide Pt(111) terraces, namely a broad and plateau-like peak. In the "double layer region" between 0.35 and 0.60 V vs RHE, a small peak is observed at 0.55 V vs RHE in the positive-going scan and 0.56 V vs RHE in the reversed scan (note the unexpected higher potential of the cathodic peak), as already reported by Feliu et al.[21] As the potential increases from 0.60 to 0.90 V vs RHE, there is a sharp peak at 0.69 V vs RHE followed by a broader feature (with the corresponding reversible features in the negative-going scan). This sharp peak has been ascribed to OH adsorption and is observed only for a Pd monolayer covering a Pt(111) substrate with very low step density, i.e. it requires wide (111) terraces.[21] The combination of a sharp and broad peak is very typical for a disorder-order transition in the adlayer,[32] but the sequence (sharp peak at low coverage, broad peak at higher coverage) is unexpected.

5.4.2 Cation and anion effects on the blank voltammogram of $Pd_{ML}Pt(111)$

Figure 5.2a shows cyclic voltammograms for the $Pd_{ML}Pt(111)$ electrode in 0.1 M $HClO_4$ (pH = 1), 0.01 M $HClO_4$ (pH = 2) and 0.001 M $HClO_4$ (pH = 3) electrolytes. On the reversible hydrogen electrode (RHE) scale, the H_I peak is observed to be independent of pH, perchlorate concentration and the ionic strength of the electrolyte solution, in acidic electrolyte (pH = 1 - 3) in the absence of alkali metal cations. As the pH lowers, or rather as the perchlorate concentration increases, peaks H_I and H_{II} start overlapping more and more as shown in Figure 5.2b. Figure 5.2c and d illustrate that the effect of cations on the H_I peak of the $Pd_{ML}Pt(111)$ electrode becomes apparent when voltammograms are recorded in 0.001 M $HClO_4$ (pH = 3) with different amounts of alkali perchlorate salts. With increasing concentration of alkali metal cation, the H_I peak shifts to more positive potential in comparison with the peak potential (0.246 V vs RHE) in 0.001 M $HClO_4$ without alkali cations. The shift is more pronounced for larger cations: for 0.01 M Li^+ (Figure 5.2c) and 0.01 M Na^+ (Figure 5.2d) containing electrolytes, the H_I peak is shifted to 0.262 and 0.272 V vs RHE, respectively. This effect of the cation on the peak potential is identical to the effect that we observed previously for the step-related "hydrogen" peaks on stepped Pt electrodes.[4,5]

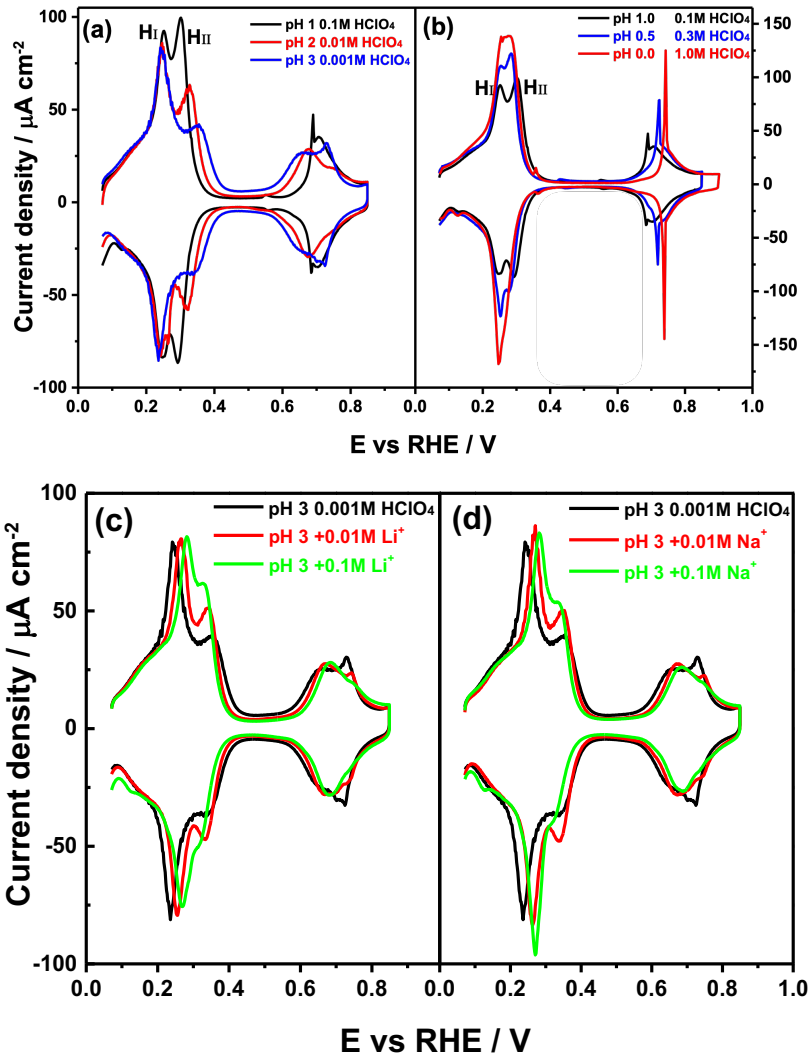

FIGURE 5.2

Cyclic voltammograms of $Pd_{ML}Pt(111)$ in (a) 0.1 M $HClO_4$ (pH = 1), 0.01 M $HClO_4$ (pH = 2) and 0.001 M $HClO_4$ (pH = 3) solutions and (b) 0.1 M $HClO_4$ (pH = 1), 0.5 M $HClO_4$ (pH = 0.3) and 1.0 M $HClO_4$ (pH = 0) solutions. (c) and (d) 0.001 M $HClO_4$ (pH = 3) solution without and with $MeClO_4$, where Me is Li and Na, as indicated. Scan rate: 50 mV s^{-1}.

Therefore, we conclude that, similarly to the stepped Pt electrodes, the H_I peak involves the replacement of H_{ads} by OH_{ads} and this adsorbate replacement reaction is driven to more positive potentials due to the destabilizing effect of the co-adsorbed alkali cation on hydroxyl adsorption.[4,5,33] At constant pH, the adsorption of alkali cations on the $Pd_{ML}Pt(111)$ surface becomes more favorable

with increasing cation concentration, resulting in a greater shift of the H_I peak, as shown in Figure 5.2c and d. A reaction equation of the H_I reduction/oxidation peak on $Pd_{ML}Pt(111)$ can thus be formally written as:

$$x(OH_{ads} - cation_{ads}) + (1+x)H^+ + (1+x)e^- \rightleftarrows H_{ads} + xH_2O + x(cation_{sol}) \qquad 5.1$$

Remarkably, Figure 5.2 shows that the H_{II} peak does not show the same cation effect as the H_I peak. By contrast, the H_{II} peak is sensitive to anion concentration (and identity, as shown in Figure 5.3) and the pH of the electrolyte. Figures 2a and b show that the H_{II} peak becomes sharper and shifts to lower potential with increasing $HClO_4$ concentration. For clarity, we show representative voltammograms of $Pd_{ML}Pt(111)$ in Figure 5.2b; results obtained in electrolytes with detailed wider range of pH values are shown in Figure D2 in Appendix D. Figure 5.2c and d (and Figure D2) show that the shift in the H_{II} peak seems to be at least partially due to different perchlorate concentration, as at constant pH the H_{II} peak grows with increasing perchlorate concentration and also shows a negative potential shift. Another important observation from Figure 5.2 is that the voltammetric feature between 0.60 to 0.90 V vs RHE is sensitive to the $HClO_4$ concentration. This feature shifts to a higher potential in the presence of a higher concentration of perchlorate, suggesting that the formation of the adsorbate in this potential window is inhibited by the presence of perchlorate. A consistent explanation for this effect of perchlorate, which will be considered for the remainder of this ***Chapter***, is that the H_{II} peak involves either the specific adsorption of perchlorate, or a strong interaction of perchlorate with the other adsorbates. If OH_{ads} is formed in the H_I peak (Eq. 5.1), then a reaction equation describing the H_{II} peak could formally read as:

$$x(OH_{ads} - cation_{ads}) + x(H^+ + e^-) + y\,(anion_{sol}) \rightleftarrows xH_2O + y\,(anion_{ads}) + x\,(cation_{sol}) \qquad 5.2$$

In this equation, the extent of anion adsorption is influenced by the anion concentration, but also by the pH, as the potential of zero charge (E_{pzc}) shifts to higher potential on the RHE scale with increasing pH, enhancing perchlorate adsorption at a given potential on the RHE scale.

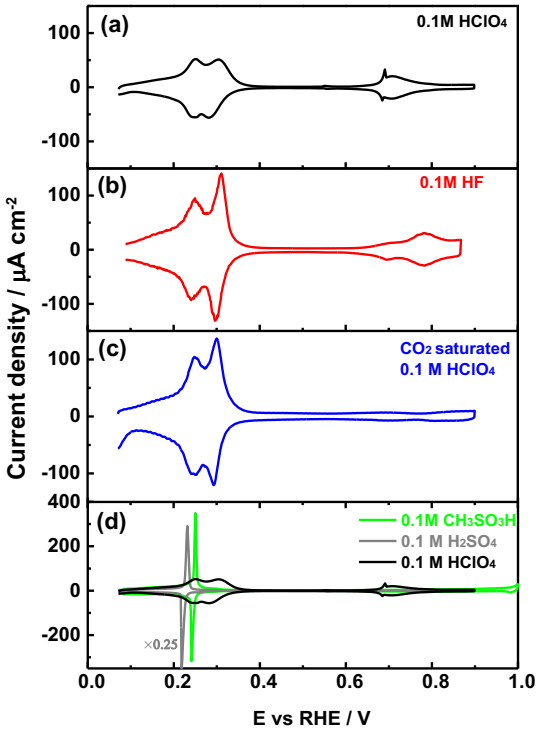

FIGURE 5.3

Cyclic voltammogram of $Pd_{ML}Pt(111)$ recorded in (a) 0.1 M $HClO_4$, (b) 0.1 M HF, (c) CO_2 saturated 0.1 M $HClO_4$ solution, and (d) 0.1 M CH_3SO_3H. Scan rate: 50 mV s^{-1}.

To explore the anion effect on the H_{II} peak further, Figure 5.3 shows the voltammetry for different anions. In agreement with Figure 5.2, there is no impact of the anion on the H_I peak in the presence of F^- (Figure 5.3b) and HCO_3^- (Figure 5.3c), which suggests that anion adsorption or interaction is insufficient to perturb the OH_{ads} in this potential window. On the other hand, the H_{II} peak is observed to increase in sharpness in 0.1 M hydrofluoric acid (HF) (Figure 5.3b) and in CO_2 saturated (Figure 5.3c) perchloric acid compared to 0.1 M $HClO_4$ solution, suggesting that F^- and HCO_3^- anion affect the shape of the H_{II} peak. The role of anion adsorption is also reflected in the marked competitive adsorption with the adsorption states between 0.60 and 0.90 V vs RHE: in 0.1 M HF, these states are suppressed compared to 0.1 M $HClO_4$ solution, whereas in CO_2 saturated 0.1 M $HClO_4$ solution these states are blocked completely by adsorbed bicarbonate, just as in sulfuric acid (as shown in Figure 5.1a). Spectro-electrochemical experiments have shown that the bands corresponding to adsorbed bicarbonate on $Pd_{ML}Pt(111)$ surface appear at 0.40 V vs RHE, i.e. in the beginning of the "double-layer" window.[34]

The voltammograms of Pt(111) in 0.1 M CH_3SO_3H and $HClO_4$ electrolytes have been observed to be very similar, showing that both are non-specifically adsorbing electrolytes on Pt(111),[35] see also Figure D3. Surprisingly, the cyclic voltammogram shown in Figure 5.3d strongly suggests the methanesulfonate

anion from the CH_3SO_3H electrolyte behaves similar to the 0.1 M H_2SO_4 solution, and, therefore, methanesulfonate must be strongly adsorbed on the $Pd_{ML}Pt(111)$ electrode surface at low potentials. These results suggest that the SO_3 from (bi)sulphate/CH_3SO_3H adsorbs more strongly on the Pd surface than on Pt. For such strong anion adsorption, reactions 1 and 2 are replaced by:

$$H_{ads} + y\,(anion) \rightleftarrows H^+ + e^- + y\,(anion_{ads}) \qquad 5.3$$

It may be that a small concentration of Cl^- preexists as a trace impurity in $HClO_4$ and/or is generated by the reduction of perchlorate ions catalyzed by palladium.[22] In order to eliminate the possibility of chloride present in $HClO_4$ being responsible for the H_{II} peak, small amounts (10^{-6} and 10^{-5} M) of Cl^- were intentionally added to 0.1 M $HClO_4$ (pH = 1) and 0.001 M $HClO_4$ (pH = 3) solutions, respectively. Figure D4 in Appendix D shows the change caused by Cl^-: the H_I and H_{II} peaks exhibit some asymmetry, in contrast to the symmetric peaks observed in solutions containing only $HClO_4$. This observation makes it highly unlikely that the H_{II} peak is related to the presence of chloride anions.

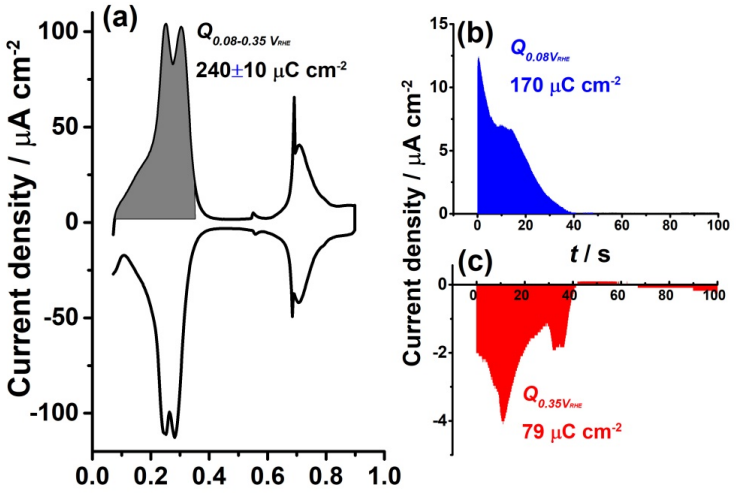

FIGURE 5.4

(a) Cyclic voltammogram of $Pd_{ML}Pt(111)$ recorded in (a) 0.1 M $HClO_4$; current-time transients recorded during CO adsorption/displacement at (b) 0.08 V vs RHE and (c) 0.35 V vs RHE in 0.1 M $HClO_4$.

To further elucidate the nature of the adsorption-desorption process in the hydrogen region at the $Pd_{ML}Pt(111)$/electrolyte interface in perchloric acid, CO displacement experiments were performed. For the CO displacement experiment, CO was added to the solution and its adsorption at the electrode surface at fixed potential leads to a current transient related to the displacement of species adsorbed on the surface in the absence of CO. The total surface charge

at a chosen potential can be determined by integrating the transients.[26] At the threshold of hydrogen evolution, i.e. at ca. 0.08 V vs RHE, the maximum charge density corresponding to the displacement of adsorbed hydrogen is obtained.[36] As can be seen from Figure 5.4b, the transient current is positive which points to the oxidative desorption of H_{upd}:

$$H_{upd} - Pd_{ML}Pt(111) + CO \rightarrow CO - Pd_{ML}Pt(111) + H^+ + e^- \qquad 5.4$$

The H_{upd} coverage at 0.08 V vs RHE is then estimated to be $170/250 \approx 0.68$ ML. Correspondingly, at 0.35 V vs RHE negatively charged anions A are reductively displaced by CO following the reaction equation:

$$\mathrm{A} - \mathrm{P}d_{ML}\mathrm{Pt}(111) + \mathrm{CO} + e^- \rightarrow CO - \mathrm{P}d_{ML}\mathrm{Pt}(111) + A^- \qquad 5.5$$

The result shows good agreement between the charge density values obtained from the integration of the transient current response (249 μ C cm^{-2}) and of the voltammetric profile characteristic (240±10 μ C cm^{-2}) of the $Pd_{ML}Pt(111)$ interface. The reductive desorption of anions (as shown in Figure 5.4c) indeed indicates that adsorbed anions are involved in the H_{II} peak and the calculated Θ_A on $Pd_{ML}Pt(111)$ at the low potential region in 0.1 M $HClO_4$ is around 0.33 ML, according to the coulometric estimation.

5.4.3 Thermodynamics of *H, *OH + *H_2O, *O, *ClO_4, *SO_4 and *HSO_4 adsorption

Figure 5.5a and b show the experimentally measured cyclic voltammograms (upper panel) of Pt(111) and $Pd_{ML}Pt(111)$ in 0.1 M $HClO_4$ along with the DFT-calculated free energies of adsorption of hydrogen, hydroxide, oxygen, and perchlorate as a function of potential vs RHE (lower panel). The lower panel shows the most stable coverages at any given potential (for more details, see Appendix D). The coverages investigated with DFT are: hydroxide from 2/9 to 2/3 ML for Pt(111) and from 1/9 to 2/3 ML for $Pd_{ML}Pt(111)$, hydrogen from 1/9 to 1 ML for both Pt(111) and $Pd_{ML}Pt(111)$, from 1/9 to 2/3 ML for oxygen on both Pt(111) and $Pd_{ML}Pt(111)$, and 1/9 ML of perchlorate on both surfaces. The black horizontal line at 0 eV represents the reference state of the bare surface and the red line represents the adsorption of perchlorate.

It is important to consider the adsorption of water onto the electrode surface, as its adsorption could compete with that of hydrogen and hydroxide. However, given that the adsorption of water depends strongly on van der Waals (vdW) interactions, and these interactions are poorly captured with DFT-GGAs,[37] an accurate calculation of the adsorption energy of water is difficult. This is important not only for considering water adsorption, but also for the effects of co-adsorbed water on hydroxide adsorption. We therefore used three methods to evaluate the adsorption of water and its effect on our conclusions, primarily on the adsorption thermodynamics of solvated *OH: (1) a combined PBE and empirical vdW correction with PBE-D3[38,39] only on the adsorption of *OH + *H_2O and *H_2O using solution-phase water as the reference state. (2) Using only PBE with the adsorbed water adlayer as the reference state for hydroxide adsorption

where the error in the adsorption energy of the water bilayer in the reactant state, and that of the partial bilayer in the *OH +*H_2O product state, may partially cancel out.[40,41] (3) Using empirical vdW corrections with PBE-D3 for all adsorbates, *H, *H_2O, *OH+*H_2O and *O, and solution-phase water as the reference state.

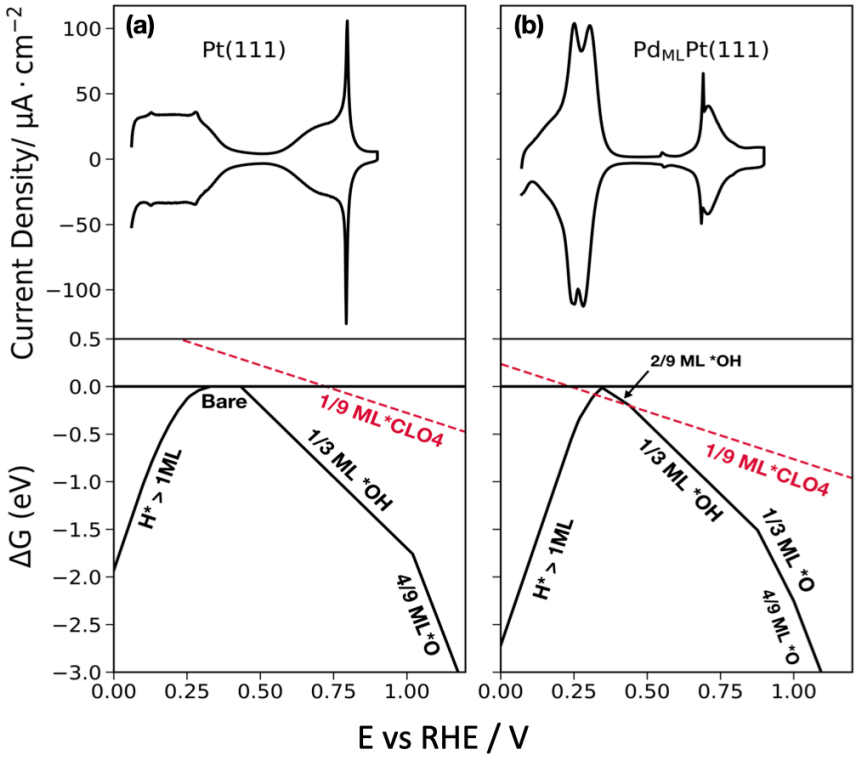

FIGURE 5.5

Upper panels are the cyclic voltammograms of (a) Pt(111) and (b) $Pd_{ML}Pt(111)$) in 0.1 M $HClO_4$ recorded at 50 mV s^{-1}. Black lines in the lower panels show the most stable adsorption free energies and the most favorable coverages as a function of potential for the adsorption of hydrogen (*H), hydroxide (*OH) and oxygen (*O). Perchlorate adsorption (*ClO_4) is shown in red at a 1/9 ML coverage.

The phase diagrams obtained with the different methods 1, 2 and 3 for $Pd_{ML}Pt(111)$ and Pt(111) are shown in Appendix D, Figures D6 and D7. In general, all the methods show similar trends of *H, *OH + *H_2O and *O adsorption. We have decided to base our conclusion on results derived from method 2 (shown in Figure 5.5) as it is simple and captures well the trends compared to experiment. For Pt(111) and $Pd_{ML}Pt(111)$, the trends obtained with method 2 and 3 are comparable to each other, as the adsorption energies and the overall trend does not significantly change as shown in Figures D6 b, c and D7 b, c. In the case of method 1, the only difference observed is the adsorption of water on $Pd_{ML}Pt(111)$ appearing at a lower potential than that of hydroxide *OH, in contrast to method

2 and 3 where hydrogen adsorption (*H) is followed by the adsorption of hydroxide (*OH). In all cases, the calculated adsorption potential of hydroxide lies around 0.3-0.4 V vs RHE for $Pd_{ML}Pt(111)$ and 0.38-0.40 V vs RHE for Pt(111). Generally, PBE tends to overestimate binding energies,[42,43] which explains why the hydroxide adsorption potentials are more negative than the experimentally measured potentials. A more detailed description of the calculation of the free energies of adsorption of hydroxide can be found as "Adsorption Free energies of *OH, *H and *O" in Figure D5 in Appendix D.

Taking Pt(111) as a reference case (for which the adsorption thermodynamics of hydrogen, hydroxide, and oxygen are known), the surface composition as a function of potential (Figure 5.5a, lower panel) matches semi-quantitatively the experiments (Figure 5.5a, upper panel). DFT results show that the broad peak at low potentials corresponds with hydrogen adsorption at full monolayer coverage below 0.33 V vs RHE followed by the double layer region (where water is adsorbed), followed by 1/3 ML hydroxide adsorption at 0.43 V vs RHE and, finally, oxygen adsorption at 4/9 ML coverage at 1.02 V vs RHE. The results shown in Figure 5.5a for Pt(111) agree with previously calculated energy diagrams of Pt(111)[19] with small differences in absolute values due to the different functional used. Including configurational entropy for the adsorbed species would probably bring the computational results in closer agreement with experiment. This is shown for hydrogen adsorption on Pt(111) and Pt(100) where a comparison of the slopes and intercept given by the relationship between the adsorption free energy as a function of coverage, including configurational entropy resulted in adsorption potentials closer to those obtained experimentally.[33] Furthermore, Karlberg et al. show how including lateral interaction of hydrogen adsorbed species and configurational entropies is important for simulating cyclic voltammograms of the hydrogen adsorption and desorption process.[44]

Figure 5.5b shows the calculated phase diagram of $Pd_{ML}Pt(111)$ (lower panel). At potentials below 0.34 V vs RHE, hydrogen is adsorbed on the surface at 1ML coverage; hydroxide adsorption happens at 0.35 V vs RHE at 2/9 ML coverage followed by 1/3 ML hydroxide adsorption at 0.44 V vs RHE. At higher potentials oxygen adsorption becomes favorable at 0.88 V vs RHE at 1/3 ML coverage and at 1.0 V vs RHE at 4/9 ML coverage. Compared to Pt(111), oxygen adsorbates bind stronger on the $Pd_{ML}Pt(111)$ surface. As will be discussed in the following sections, the DFT results support the conclusion from the previous section that the low potential peaks ($H_I + H_{II}$) correspond to an exchange between adsorbed hydrogen and adsorbed anions (*OH + $*H_2O$, $*ClO_4$). From the DFT modelling alone, it is unclear what species is adsorbed in the high potential peak (0.65-0.8 V vs RHE) observed in experiment, because oxygen adsorption is predicted to occur at potentials more positive of this peak. Therefore, if oxygen adsorption does not occur in that region, backed up by experimental results, that leaves the species present in the high potential peak as $*ClO_4$, *OH or a mixed adlayer of the two. The charge in this high potential peak is then most likely due to either an increase in the adsorbed hydroxide coverage (within a mixed perchlorate/hydroxide adlayer) or a replacement of perchlorate with a higher coverage of adsorbed hydroxide, as we expect adsorbed perchlorate to keep some of its charge (as seen for adsorbed (bi)sulfate, for example) and exhibit repulsive interactions.

5.4.4 Anion adsorption

To further understand the anion effect on the H_I and H_{II} region observed in the experiments, we investigated the adsorption thermodynamics of various anions, *ClO_4, *HSO_4, *SO_4, *F, and *HCO_3 on Pt(111) and Pd_{ML}Pt(111). Adsorption of these anions was considered only at low coverage of 1/9 ML and explicitly solvated with 1 water molecule for each of the anions except for *F where 2 water molecules were used and for *OH where a partially dissociated water bilayer (1/3*OH-1/3*H_2O) solvation was used. We will first discuss the main results obtained for *ClO_4, *HSO_4 and *SO_4 and then we will show a comparison between the binding strength of *ClO_4, *HSO_4, *SO_4, *F, and *HCO_3 anions on Pd_{ML}Pt(111) compared to that of Pt(111).

Obtaining an accurate adsorption potential for anions such as ClO_4^-, SO_4^{2-} and HSO_4^- depends on how accurate their solution-phase free energy is determined. There are many methods which could be used to calculate the solution-phase free energy, including thermodynamic cycles which avoid the need to correctly capture the solvation energy of the anion with traditional DFT techniques, which is a difficult task because of the long length and time scales of important solvation dynamics. However, to take those into account molecular dynamics simulations are preferred.[45,46] Here, the solution-phase free energy of perchlorate, sulfate and bisulfate was calculated as described in ***Chapter 3***. Briefly, the free energy of the aqueous anion is determined by using the calculated DFT energy of a neutral species (typically in the gas phase), that upon reduction produces the target anion, and by using the half-redox equilibrium potential at which this reduction reaction occurs, we can easily calculate the free energy of the solution-phase anion. This method is analogous to the computational hydrogen electrode method (CHE)[27] for calculating the free energy of protons in solution, but in the case of hydrogen/protons, the equilibrium potential is defined to be exactly 0 V vs SHE and is not experimentally measured.[47–49] For more detailed and robust methods to determine solution-phase free energies and simulate CVs see ref.[50,51]

Our DFT results show that the adsorption potential at which perchlorate binds on the Pd_{ML}Pt(111) at 1/9 ML coverage overlaps with that of low coverages of hydrogen *H at 0.32 V vs RHE and with *OH at 0.44 V vs RHE V, as shown by the red line in Figure 5.5b (lower panel). The adsorption potential of perchlorate on Pt(111) lies at more positive potentials around 0.72 V vs RHE than the calculated adsorption of 1/3 ML hydroxide *OH, which occurs at around 0.43 V vs RHE. This suggests that perchlorate adsorbs more strongly on Pd_{ML}Pt(111) than on Pt(111), and could outcompete hydroxyl adsorption and even low-coverage hydrogen adsorption on Pd_{ML}Pt(111). Conversely, on Pt(111) hydroxyl outcompetes perchlorate adsorption. Furthermore, at higher potentials, after ~0.55 V vs RHE, a perchlorate-hydroxyl mixed adlayer could form, and as the potential is increased this mixed adlayer can either (i) co-adsorb higher *OH coverages with *ClO_4, or (ii) higher coverages of *OH displace *ClO_4 from the mixed adlayer leaving an adlayer of just high-coverage *OH. This is in good agreement with our interpretation of the experimental voltammetry.

However, as we are unsure of the absolute accuracy of our calculated perchlorate adsorption potentials (in contrast to hydroxyl, for example, where we know at which potentials it adsorbs on Pt(111) from experiment), it is difficult to know if we should expect perchlorate adsorption before hydroxyl adsorption on the Pd_{ML}Pt(111) from our DFT calculations alone. Taking again Pt(111) as a benchmark, there is some experimental spectroscopic evidence interpreted to

show both that perchlorate affects hydroxyl adsorption on Pt(111)[52] and/or even specifically adsorbs in the double layer/hydroxide/oxide regions (~0.4-0.8 V vs RHE).[53] More recent studies by Attard et al.[54] show the double layer and hydroxyl adsorption regions of cyclic voltammograms measured on Pt(111) are sensitive to the perchlorate concentration, suggesting that perchlorate strongly interacts with the surface.

Therefore, considering only our DFT results, there is computational support that the low potential peak in the CV measured on $Pd_{ML}Pt(111)$ (comprising both H_I and H_{II} in Figure 5.1b) corresponds to an exchange between *H / *OH+*H_2O and *ClO_4 as seen in Figure 5.2b and Figure 5.5b (lower panel), and is, therefore, not solely due to hydrogen adsorption, consistent with the conclusions from the experimental voltammograms, CO displacement measurements, and cation/anion/pH effects. The total coverage of hydrogen and anion (*OH) adsorption matches that measured by *CO displacement (Figure 5.4b and c). However, we have calculated a *H coverage of 1 ML adsorbed at low potentials (at the lower potential limit of the CV), and CO displacement gives an *H coverage of ~0.71 ML. This discrepancy could be due to the omission of configurational entropy for the calculation of the free energy, which would make high-coverage *H adsorption less favorable than calculated here.

Additionally, we compared the calculated adsorption potentials of *SO_4 with the CV of Pt(111) and the adsorption potential of *SO_4 and *HSO_4 with the CV of $Pd_{ML}Pt(111)$ as measured in 0.1 M H_2SO_4, see Figure 5.6. The calculated adsorption potential of sulfate on Pt(111) is 0.57 V vs RHE, falling in the high potential region of the CV where sulfate/bisulfate adsorption is known to occur on Pt(111).[55–59] Significant debate has centered on which anion (bisulfate vs. sulfate) corresponds to this adsorption peak in the cyclic voltammogram; given our limited investigation of the coverage dependence and the effect of solvation near the electrode surface, we do not intend to answer this question here, and take this result to be indicative of (bi)sulfate adsorption. For $Pd_{ML}Pt(111)$, the calculated bisulfate and sulfate adsorption potentials are 0.47 V vs RHE and 0.45 V vs RHE respectively, in both cases falling in the region where (bi)sulfate is adsorbed on the surface fully blocking active sites. Similar to Pt(111), this peak has been assigned to bisulfate/sulfate anions based on the spectroscopic data obtained by in situ FTIR experiments.[21] It is important to note that with our DFT model employed here we cannot specify which anion adsorbs more preferably in the bisulfate/sulfate region on both surfaces. This model could be improved by examining additional coverages of (bi)sulfate/sulfate, water solvation and also by specifying a more accurate solution-phase reference state for the anions.[60,61]

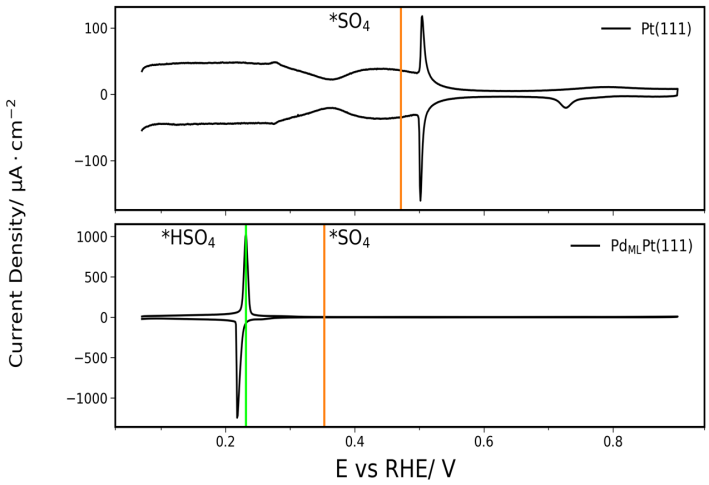

FIGURE 5.6

Cyclic voltammograms of Pt(111) and $Pd_{ML}Pt(111)$ in 0.1M H_2SO_4 recorded at 50 mV s^{-1} along with the DFT calculated adsorption potentials for $*SO_4$ in orange and $*HSO_4$ in green.

We found that in general, anions bind more strongly to the $Pd_{ML}Pt(111)$ surface than on Pt(111). This is shown in Figure 5.7, where the DFT-calculated relative free energies of adsorption with respect to Pt(111) are shown. Such a comparison of adsorption strength between $Pd_{ML}Pt(111)$ and Pt(111) is not dependent on the energy of the solution-phase anion. For all the adsorbates studied, with the exception of *OH in vacuum, the binding energy is stronger on $Pd_{ML}Pt(111)$. The bars in orange represent the adsorbed anion without solvation and the bars in blue represent the adsorbed anion with water solvation. We use one explicit water molecule for all adsorbates, except for *OH which is solvated as a 1/3*OH-1/3 $*H_2O$ bilayer, and for fluoride which is solvated by two water molecules. It is interesting to note that for most of the adsorbates the solvation effect is more predominant on $Pd_{ML}Pt(111)$, as noted by the more negative energy for the anion solvated with respect to that in vacuum. However, for bisulfate in the bidentate configuration, $*HSO_4$ bid., bicarbonate $*HCO_3$, and fluoride *F the solvation effect is slightly more predominant on Pt(111), by ~0.04 eV, ~0.05 eV and ~0.04 eV, respectively, as observed by the less negative energy difference of the solvated anion compared to the conditions in vacuum.

Interestingly, we also find that water binds more strongly to $Pd_{ML}Pt(111)$ than to Pt(111). A single water molecule (at 1/9 ML coverage) binds ~0.15 eV stronger and within a 2/3 ML water adlayer the binding strength per water molecule is ~0.03 eV stronger on the $Pd_{ML}Pt(111)$ compared to Pt(111). This suggests that the typically stronger adsorption seen for the anions on $Pd_{ML}Pt(111)$ with solvation vs. without solvation may be simply due to a stronger adsorption of water on the $Pd_{ML}Pt(111)$ surface.

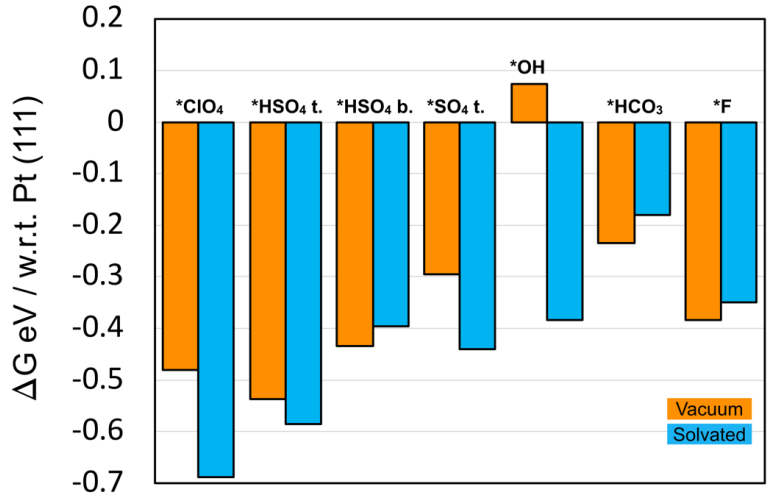

FIGURE 5.7

Relative DFT-calculated free energies on $Pd_{ML}Pt(111)$ calculated with respect to (w.r.t.) Pt(111) for perchlorate $*ClO_4$, bisulfate in tridentate configuration $*HSO_4$ t., bisulfate in bidentate configuration $*HSO_4$ b., sulfate in tridentate configuration $*SO_4$ t., hydroxyl *OH, bicarbonate $*HCO_3$ and fluoride *F. The orange bars represent the free energies in vacuum and the blue bars represent the solvated free energies.

While with DFT alone we cannot differentiate the phenomena in H_I and H_{II} separately, in conjunction with the experimentally observed pH, cation, and anion effects, we conclude that (i) the first feature in the low-potential peak on the $Pd_{ML}Pt(111)$, the region of H_I and H_{II}, is comprised of an exchange between adsorbed *H and $*OH + *H_2O$ adlayer matching the location, total charge, and ratio of *H/anion charge displaced as measured by experiment, and (ii) that this region (H_I and H_{II}) is affected by the specific adsorption of perchlorate. Additional DFT studies should be performed to further investigate the effects of perchlorate coverage, and near-surface solvation, as well as methods to accurately and reliably define the free energy of solution-phase anions, so that the competition between adsorbed hydroxide and adsorbed perchlorate can be confidently quantified.

We have also shown that our DFT model gives a good estimate of the adsorption potentials of $*SO_4$ and $*HSO_4$ on Pt(111) and $Pd_{ML}Pt(111)$, matching qualitatively those obtained experimentally, giving further semi-quantitative confidence in the perchlorate results. Lastly, in agreement with the experimental results, DFT also supports stronger anion binding on $Pd_{ML}Pt(111)$ compared to Pt(111).

Hydroxyl adsorption plays an important role in catalytic reactions such as the oxygen reduction reaction, and its adsorption trends have helped explain non-Nernstian pH dependence shifts on Pt(110) and Pt(100). Such shifts are a result of a weaker binding of *OH on the surface, due to an effect of alkali metal cations in alkaline solutions.[33] Therefore, studying *OH adsorption on the $Pd_{ML}Pt(111)$, allows us to explain CV features and can provide further information for mechanistic studies where binding of *OH species serve as descriptor for catalytic

activity such as oxygen reduction. Similarly, anion adsorption is important for catalytic reactions such as formic acid oxidation, where it has been shown that the presence of pre-adsorbed sulfate induces a lower onset potential on Pt(111).[62] On Pd thin films, formic acid oxidation is suppressed by sulfate/bisulfate anions and CO formation is enhanced.[63] Beyond catalytic reactions, specific adsorption of anions are of particular interest in studies of surface structure.[64,65]

5.5 Conclusions

In this ***Chapter***, we identified the adsorption processes taking place in the various peaks of the blank voltammogram of the well-defined $Pd_{ML}Pt(111)$ surface in perchloric acid by means of experimental and computational studies. We showed that:
(i) The "first hydrogen peak" H_I at 0.246 V vs RHE is not due to just adsorption and desorption of hydrogen, but actually involves the replacement of hydrogen by hydroxyl. The hydroxyl adsorption is sensitive to the nature of the electrolyte cation, in agreement with our previous work on stepped Pt electrodes.
(ii) The "second hydrogen peak" H_{II} at 0.306 V vs RHE involves the exchange of *H/*OH to adsorbed perchlorate $*ClO_4$. The coverage of the adsorbed perchlorate, can be assumed to be 1/3 ML on $Pd_{ML}Pt(111)$ at the positive end of the H_{II} peak. If more strongly adsorbed anions are added to the electrolyte, the H_I and H_{II} peaks merge, and the high potential adsorption states are blocked; that is, strongly adsorbed anions suppress OH/O adsorption at both lower and higher potentials. In strong contrast to Pt(111), we have not identified any anion that we can safely assume to be not adsorbed specifically on $Pd_{ML}Pt(111)$.

We believe that these detailed insights will be very important in correctly interpreting and understanding the catalytic properties of palladium and palladium-modified electrodes.

5.6 References

(1) Strmcnik, D.; Kodama, K.; Vliet, D. van der; Greeley, J.; Stamenkovic, V. R.; Marković, N. M. The Role of Non-Covalent Interactions in Electrocatalytic Fuel-Cell Reactions on Platinum. *Nature Chem* **2009**, *1* (6), 466–472.

(2) Magnussen, O. M. Ordered Anion Adlayers on Metal Electrode Surfaces. *Chem. Rev.* **2002**, *102* (3), 679–726.

(3) Tripkovic, D. V.; Strmcnik, D.; van der Vliet, D.; Stamenkovic, V.; Markovic, N. M. The Role of Anions in Surface Electrochemistry. *Faraday Discuss.* **2009**, *140* (0), 25–40.

(4) Chen, X.; McCrum, I. T.; Schwarz, K. A.; Janik, M. J.; Koper, M. T. M. Co-Adsorption of Cations as the Cause of the Apparent PH Dependence of Hydrogen Adsorption on a Stepped Platinum Single-Crystal Electrode. *Angew. Chem. Int. Ed* **2017**, *56* (47), 15025–15029.

(5) McCrum, I. T.; Chen, X.; Schwarz, K. A.; Janik, M. J.; Koper, M. T. M. Effect of Step Density and Orientation on the Apparent PH Dependence of Hydrogen and Hydroxide Adsorption on Stepped Platinum Surfaces. *J. Phys. Chem. C* **2018**, *122* (29), 16756–16764.

(6) Clavilier, J.; Armand, D.; Sun, S. G.; Petit, M. Electrochemical Adsorption Behaviour of Platinum Stepped Surfaces in Sulphuric Acid Solutions. *J. Electroanal. Chem. Interf. Electrochem.* **1986**, *205* (1), 267–277.

(7) Chen, X.; Koper, M. T. M. Mass-Transport-Limited Oxidation of Formic Acid on a PdMLPt(100) Electrode in Perchloric Acid. *Electrochem. commun.* **2017**, *82*, 155–158.

(8) Arenz, M.; Schmidt, T. J.; Wandelt, K.; Ross, P. N.; Markovic, N. M. The Oxygen Reduction Reaction on Thin Palladium Films Supported on a Pt(111) Electrode. *J. Phys. Chem. B* **2003**, *107* (36), 9813–9819.

(9) Arenz, M.; Stamenkovic, V.; Ross, P. N.; Markovic, N. M. Surface (Electro-)Chemistry on Pt(111) Modified by a Pseudomorphic Pd Monolayer. *Surf. Sci.* **2004**, *573* (1), 57–66.

(10) Kortlever, R.; Balemans, C.; Kwon, Y.; Koper, M. T. M. Electrochemical CO2 Reduction to Formic Acid on a Pd-Based Formic Acid Oxidation Catalyst. *Catal. Today* **2015**, *244*, 58–62.

(11) Min, X.; Kanan, M. W. Pd-Catalyzed Electrohydrogenation of Carbon Dioxide to Formate: High Mass Activity at Low Overpotential and Identification of the Deactivation Pathway. *J. Am. Chem. Soc.* **2015**, *137* (14), 4701–4708.

(12) Armstrong, F. A.; Hirst, J. Reversibility and Efficiency in Electrocatalytic Energy Conversion and Lessons from Enzymes. *Proc Natl Acad Sci USA* **2011**, *108* (34), 14049.

(13) Cuesta, A.; Kibler, L. A.; Kolb, D. M. A Method to Prepare Single Crystal Electrodes of Reactive Metals: Application to Pd(Hkl). *J. Electroanal. Chem.* **1999**, *466* (2), 165–168.

(14) Baldauf, M.; Kolb, D. M. Formic Acid Oxidation on Ultrathin Pd Films on Au(Hkl) and Pt(Hkl) Electrodes. *J. Phys. Chem.* **1996**, *100* (27), 11375–11381.

(15) Kibler, L. A.; El-Aziz, A. M.; Hoyer, R.; Kolb, D. M. Tuning Reaction Rates by Lateral Strain in a Palladium Monolayer. *Angew. Chem. Int. Ed.* **2005**, *44* (14), 2080–2084.

(16) El-Aziz, A. M.; Hoyer, R.; Kibler, L. A.; Kolb, D. M. Potential of Zero Free Charge of Pd Overlayers on Pt(111). *Electrochim. Acta* **2006**, *51* (12), 2518–2522.

(17) *Thin Films: Preparation, Characterization, Applications*; Soriaga, M. P., Stickney, J., Bottomley, L. A., Kim, Y.-G., Eds.; Springer US, 2002.

(18) Attard, G. A.; Price, R.; Al-Akl, A. Palladium Adsorption on Pt(111): A Combined Electrochemical and Ultra-High Vacuum Study. *Electrochim. Acta* **1994**, *39* (11), 1525–1530.

(19) McCrum, I. T.; Hickner, M. A.; Janik, M. J. First-Principles Calculation of Pt Surface Energies in an Electrochemical Environment: Thermodynamic Driving Forces for Surface Faceting and Nanoparticle Reconstruction. *Langmuir* **2017**, *33* (28), 7043–7052.

(20) Álvarez, B.; Climent, V.; Rodes, A.; Feliu, J. M. Anion Adsorption on Pd–Pt(111) Electrodes in Sulphuric Acid Solution. *J. Electroanal. Chem.* **2001**, *497* (1), 125–138.

(21) Alvarez, B.; Feliu, J. M.; Clavilier, J. Long-Range Effects on Palladium Deposited on Pt(111). *Electrochem. Commun.* **2002**, *4* (5), 379–383.

(22) Arenz, M.; Stamenkovic, V.; Schmidt, T. J.; Wandelt, K.; Ross, P. N.; Markovic, N. M. The Effect of Specific Chloride Adsorption on the Electrochemical Behavior of Ultrathin Pd Films Deposited on Pt(111) in Acid Solution. *Surf. Sci.* **2003**, *523* (1), 199–209.

(23) Llorca, M. J.; Feliu, J. M.; Aldaz, A.; Clavilier, J. Electrochemical Structure-Sensitive Behaviour of Irreversibly Adsorbed Palladium on Pt(100), Pt(111) and Pt(110) in an Acidic Medium. *J. Electroanal. Chem.* **1993**, *351* (1), 299–319.

(24) Hoyer, R.; Kibler, L. A.; Kolb, D. M. The Initial Stages of Palladium Deposition onto Pt(1 1 1). *Electrochim. Acta* **2003**, *49* (1), 63–72.

(25) Okada, J.; Inukai, J.; Itaya, K. Underpotential and Bulk Deposition of Copper on Pd(111) in Sulfuric Acid Solution Studied by in Situ Scanning Tunneling Microscopy. *Phys. Chem. Chem. Phys.* **2001**, *3* (16), 3297–3302.

(26) Clavilier, J.; Albalat, R.; Gomez, R.; Orts, J. M.; Feliu, J. M.; Aldaz, A. Study of the Charge Displacement at Constant Potential during CO Adsorption on Pt(110) and Pt(111) Electrodes in Contact with a Perchloric Acid Solution. *J. Electroanal. Chem.* **1992**, *330* (1), 489–497.

(27) Nørskov, J. K.; Rossmeisl, J.; Logadottir, A.; Lindqvist, L.; Kitchin, J. R.; Bligaard, T.; Jónsson, H. Origin of the Overpotential for Oxygen Reduction at a Fuel-Cell Cathode. *J. Phys. Chem. B* **2004**, *108* (46), 17886–17892.

(28) Sakong, S.; Naderian, M.; Mathew, K.; Hennig, R. G.; Groß, A. Density Functional Theory Study of the Electrochemical Interface between a Pt Electrode and an Aqueous Electrolyte Using an Implicit Solvent Method. *The Journal of Chemical Physics* **2015**, *142* (23), 234107.

(29) Sakong, S.; Groß, A. Methanol Oxidation on Pt(111) from First-Principles in Heterogeneous and Electrocatalysis. *Electrocatalysis* **2017**, *8* (6), 577–586.

(30) Garcia-Araez, N.; Lukkien, J. J.; Koper, M. T. M.; Feliu, J. M. Competitive Adsorption of Hydrogen and Bromide on Pt(100): Mean-Field Approximation vs. Monte Carlo Simulations. *J. Electroanal. Chem.* **2006**, *588* (1), 1–14.

(31) Garcia-Araez, N.; Koper, M. T. M. A Sublattice-Model Isotherm for the Competitive Coadsorption of Hydrogen and Bromide on a Pt(100) Electrode. *Phys. Chem. Chem. Phys.* **2010**, *12* (1), 143–148.

(32) Koper, M. T. M.; Lukkien, J. J. Modeling the Butterfly: Influence of Lateral Interactions and Adsorption Geometry on the Voltammetry at (111) and (100) Electrodes. *Surf. Sci.* **2002**, *498* (1), 105–115.

(33) McCrum, I. T.; Janik, M. J. PH and Alkali Cation Effects on the Pt Cyclic Voltammogram Explained Using Density Functional Theory. *J. Phys. Chem. C* **2016**, *120* (1), 457–471.

(34) Berná, A.; Rodes, A.; Feliu, J. M.; Illas, F.; Gil, A.; Clotet, A.; Ricart, J. M. Structural and Spectroelectrochemical Study of Carbonate and Bicarbonate Adsorbed on Pt(111) and Pd/Pt(111) Electrodes. *J. Phys. Chem. B* **2004**, *108* (46), 17928–17939.

(35) Sandoval-Rojas, A. P.; Gómez-Marín, A. M.; Suárez-Herrera, M. F.; Climent, V.; Feliu, J. M. Role of the Interfacial Water Structure on Electrocatalysis: Oxygen Reduction on Pt(111) in Methanesulfonic Acid. *Catal. Today* **2016**, *262*, 95–99.

(36) Orts, J. M.; Gómez, R.; Feliu, J. M.; Aldaz, A.; Clavilier, J. Potentiostatic Charge Displacement by Exchanging Adsorbed Species on Pt(111) Electrodes—Acidic Electrolytes with Specific Anion Adsorption. *Electrochim. Acta* **1994**, *39* (11), 1519–1524.

(37) Carrasco, J.; Klimeš, J.; Michaelides, A. The Role of van Der Waals Forces in Water Adsorption on Metals. *J. Chem. Phys.* **2013**, *138* (2), 024708.

(38) Grimme, S.; Antony, J.; Ehrlich, S.; Krieg, H. A Consistent and Accurate Ab Initio Parametrization of Density Functional Dispersion Correction (DFT-D) for the 94 Elements H-Pu. *J. Chem. Phys.* **2010**, *132* (15), 154104.

(39) Grimme, S.; Ehrlich, S.; Goerigk, L. Effect of the Damping Function in Dispersion Corrected Density Functional Theory. *J. Comput. Chem.* **2011**, *32* (7), 1456–1465.

(40) Granda-Marulanda, L. P.; Builes, S.; Koper, M. T. M.; Calle-Vallejo, F. Influence of Van Der Waals Interactions on the Solvation Energies of Adsorbates at Pt-Based Electrocatalysts. *ChemPhysChem* **2019**, *20* (22), 2968–2972.

(41) He, Z.-D.; Hanselman, S.; Chen, Y.-X.; Koper, M. T. M.; Calle-Vallejo, F. Importance of Solvation for the Accurate Prediction of Oxygen Reduction Activities of Pt-Based Electrocatalysts. *J. Phys. Chem. Lett.* **2017**, *8* (10), 2243–2246.

(42) Janthon, P.; Kozlov, S. M.; Viñes, F.; Limtrakul, J.; Illas, F. Establishing the Accuracy of Broadly Used Density Functionals in Describing Bulk Properties of Transition Metals. *J. Chem. Theory Comput.* **2013**, *9* (3), 1631–1640.

(43) Sun, J.; Remsing, R. C.; Zhang, Y.; Sun, Z.; Ruzsinszky, A.; Peng, H.; Yang, Z.; Paul, A.; Waghmare, U.; Wu, X.; Klein, M. L.; Perdew, J. P. Accurate First-Principles Structures and Energies of Diversely Bonded Systems from an Efficient Density Functional. *Nat. Chem.* **2016**, *8* (9), 831–836.

(44) Karlberg, G. S.; Jaramillo, T. F.; Skúlason, E.; Rossmeisl, J.; Bligaard, T.; Nørskov, J. K. Cyclic Voltammograms for H on Pt(111) and Pt(100) from First Principles. *Phys. Rev. Lett.* **2007**, *99* (12), 126101.

(45) Schnur, S.; Groß, A. Properties of Metal–Water Interfaces Studied from First Principles. *New J. Phys.* **2009**, *11* (12), 125003.

(46) Magnussen, O. M.; Groß, A. Toward an Atomic-Scale Understanding of Electrochemical Interface Structure and Dynamics. *J. Am. Chem. Soc.* **2019**, *141* (12), 4777–4790.

(47) McCrum, I. T.; Akhade, S. A.; Janik, M. J. Electrochemical Specific Adsorption of Halides on Cu 111, 100, and 211: A Density Functional Theory Study. *Electrochim. Acta* **2015**, *173*, 302–309.

(48) Gossenberger, F.; Roman, T.; Groß, A. Hydrogen and Halide Co-Adsorption on Pt(111) in an Electrochemical Environment: A Computational Perspective. *Electrochim. Acta* **2016**, *216*, 152–159.

(49) Hansen, H. A.; Man, I. C.; Studt, F.; Abild-Pedersen, F.; Bligaard, T.; Rossmeisl, J. Electrochemical Chlorine Evolution at Rutile Oxide (110) Surfaces. *Phys. Chem. Chem. Phys.* **2010**, *12* (1), 283–290.

(50) Li, Y.; Janik, M. J. Recent Progress on First-Principles Simulations of Voltammograms. *Curr. Opin. Electrochem.* **2019**, *14*, 124–132.

(51) Bagger, A.; Arán-Ais, R. M.; Stenlid, J. H.; Santos, E. C. dos; Arnarson, L.; Jensen, K. D.; Escudero-Escribano, M.; Cuenya, B. R.; Rossmeisl, J. Ab Initio Cyclic Voltammetry on Cu(111), Cu(100) and Cu(110) in Acidic, Neutral and Alkaline Solutions. *ChemPhysChem* **2019**, *20* (22), 3096–3105.

(52) Huang, Y.-F.; Kooyman, P. J.; Koper, M. T. M. Intermediate Stages of Electrochemical Oxidation of Single-Crystalline Platinum Revealed by in Situ Raman Spectroscopy. *Nat. Commun.* **2016**, *7* (1), 12440.

(53) Sawatari, Y.; Inukai, J.; Ito, M. The Structure of Bisulfate and Perchlorate on a Pt(111) Electrode Surface Studied by Infrared Spectroscopy and Ab-Initio Molecular Orbital Calculation. *J. Electron Spectrosc. Relat. Phenom.* **1993**, *64–65*, 515–522.

(54) Attard, G. A.; Brew, A.; Hunter, K.; Sharman, J.; Wright, E. Specific Adsorption of Perchlorate Anions on Pt{hkl} Single Crystal Electrodes. *Phys. Chem. Chem. Phys.* **2014**, *16* (27), 13689–13698.

(55) Braunschweig, B.; Daum, W. Superstructures and Order−Disorder Transition of Sulfate Adlayers on Pt(111) in Sulfuric Acid Solution. *Langmuir* **2009**, *25* (18), 11112–11120.

(56) Funtikov, A. M.; Stimming, U.; Vogel, R. Anion Adsorption from Sulfuric Acid Solutions on Pt(111) Single Crystal Electrodes. *J. Electroanal. Chem.* **1997**, *428* (1), 147–153.

(57) Kunimatsu, K.; Samant, M. G.; Seki, H.; Philpott, M. R. A Study of HSO4− and SO42− Co-Adsorption on a Platinum Electrode in Sulfuric Acid by in-Situ Ft-Ir Reflection Absorption Spectroscopy. *J. Electroanal. Chem. Interf. Electrochem.* **1988**, *243* (1), 203–208.

(58) Faguy, P. W.; Markovic, N.; Adzic, R. R.; Fierro, C. A.; Yeager, E. B. A Study of Bisulfate Adsorption on Pt(111) Single Crystal Electrodes Using in Situ Fourier Transform Infrared Spectroscopy. *J. Electroanal. Chem. Interf. Electrochem.* **1990**, *289* (1), 245–262.

(59) Clavilier, J. The Role of Anion on the Electrochemical Behaviour of a {111} Platinum Surface; an Unusual Splitting of the Voltammogram in the Hydrogen Region. *J. Electroanal. Chem. Interf. Electrochem.* **1980**, *107* (1), 211–216.

(60) Santana, J. A.; Cabrera, C. R.; Ishikawa, Y. A Density-Functional Theory Study of Electrochemical Adsorption of Sulfuric Acid Anions on Pt(111). *Phys. Chem. Chem. Phys.* **2010**, *12* (32), 9526–9534.

(61) Yeh, K.-Y.; Restaino, N. A.; Esopi, M. R.; Maranas, J. K.; Janik, M. J. The Adsorption of Bisulfate and Sulfate Anions over a Pt(111) Electrode: A First Principle Study of Adsorption Configurations, Vibrational Frequencies and Linear Sweep Voltammogram Simulations. *Catal. Today* **2013**, *202*, 20–35.

(62) Perales-Rondón, J. V.; Herrero, E.; Feliu, J. M. Effects of the Anion Adsorption and PH on the Formic Acid Oxidation Reaction on Pt(111) Electrodes. *Electrochim. Acta* **2014**, *140*, 511–517.

(63) Miyake, H.; Okada, T.; Samjeské, G.; Osawa, M. Formic Acid Electrooxidation on Pd in Acidic Solutions Studied by Surface-Enhanced Infrared Absorption Spectroscopy. *Phys. Chem. Chem. Phys.* **2008**, *10* (25), 3662–3669.

(64) Vasiljevic, N.; Wood, M.; Heard, P. J.; Schwarzacher, W. The Influence of Specific Anion Adsorption on the Surface Roughness of Electrodeposited Polycrystalline Cu Films. *J. Electrochem. Soc.* **2010**, *157* (4), D193–D198.

(65) Zei, M. S.; Qiao, G.; Lehmpfuhl, G.; Kolb, D. M. The Influence of Anions on the Structure of Underpotentially Deposited Cu on Au(111): A LEED, RHEED and AES Study. *Ber. Bunsenges. Phys. Chem.* **1987**, *91* (4), 349–353.

[This page is intentionally left blank]